



FE MODELLING TIBIA BONE VIBRATION - THE INFLUENCE OF SHAPE, TWIST, AND SIZE

Jamie Scanlan^{1*} Olga Umnova¹ Francis Li¹

¹ School of Science, Engineering & Environment, University of Salford, UK

ABSTRACT

The vibration response of bone has the potential to be used as a measure of bone strength for Osteoporosis detection. Modelling the vibration response requires capturing the shape of the long bones which have several complicated features. Yet modelling entire long bones does not give enough insight into the influence these features have on the vibration response. This paper identifies the key features of the shape of a tibia bone (cross-sectional shape, twist, and scale) and investigates their individual and combined effect on the eigenfrequencies of a series of finite element models. The cross-sectional shape is adjusted by changing a few key parameters defining the shape. The twist is added across the long axis of the model producing an inline twist across the length of the bone. The scale of the cross section is changed along the length of the bone to encompass the larger proximal and distal end of the long bones. The results are discussed in the context of understanding the fundamental effects of the bone's shape and generating datasets for machine learning algorithms.

Keywords: bone, modelling, osteoporosis, shape

1. INTRODUCTION

Osteoporosis is a medical term to describe the loss of bone strength and the increased risk of fracture from small falls. A possible method of measuring bone strength is to use the vibration of long bones which is directly linked to the bone stiffness, a major factor in strength [1,2]. There have been several attempts to model the vibration of long bone

*Corresponding author: j.p.scanlan@salford.ac.uk

Copyright: ©2023 Jamie Scanlan et al. This is an open-access article distributed under the terms of the Creative Commons Attribution 3.0 Unported License, which permits unrestricted use, distribution, and reproduction in any medium, provided the original author and source are credited.

involving Finite Element [FE] method to account for the shape's influence on bone vibration [3-5] but although FE models have become more detailed, few researchers have attempted to isolate particular features of the shape and/or their influence on the modal response. This paper will attempt to identify, isolate, and analyse the major features of the shape of long bones.

2. THEORY

The equation of motion for Timoshenko beams is

$$m \frac{\partial^2 y}{\partial t^2} + EI \frac{\partial^4 y}{\partial x^4} - \rho I \left(1 + \frac{E}{k'G}\right) \frac{\partial^4 y}{\partial x^2 \partial t^2} + \frac{\rho I}{k'G} \frac{\partial^4 y}{\partial t^4} = 0 \quad (1)$$

where:

$y(x, t)$ is transverse displacement with x being the distance along the axis of the beam, t the time, y the vertical and z the lateral dimensions (replacing y with z in (1) gives equation for the lateral displacement), m is the mass, which is

$$m = \rho A \quad (2)$$

where:

ρ is the surface density, A is cross sectional area; EI is the stiffness term (bending rigidity), with E the Young's/elastic modulus and I the mass moment of inertia, also known as the 2nd moment of inertia. Particular to Timoshenko beams, G is the elastic shear modulus and k' is the shape or shear correction factor, that depends on the geometry of the beam and the Poisson ratio ν . These last two terms are included to account for the shear deformation and rotary inertia effects on beam vibration. This equation can be solved semi-analytically to give the roots for free-free conditions [6]. These roots γ_n are related to the natural frequencies F_n through the following equation:

$$F_n = \frac{\gamma_n^2}{2\pi L^2} \sqrt{\frac{EI}{\rho A}} \quad (3)$$

Where L is the length of the beam. The modal frequencies are therefore directly influenced by changes in the stiffness

and the density of the material. The stiffness is itself influenced by changes to elastic modulus and the 2nd moments of inertia I , defined as:

$$I_y = \iint_R y^2 dA \quad (3.1)$$

$$I_z = \iint_R z^2 dA \quad (3.2)$$

Where: R is the region representing the cross-section. The area moment of inertia is typically different in the y and z directions and depends on the choice of reference point. In this paper, the reference point is the centroid of the cross-sectional shape R .

3. COMSOL EXPERIMENTS

A femur .stl and tibia .stl model were imported into COMSOL 6.0 with the mesh simplified using the default settings [7,8]. The models were then transformed to remove any position offsets and have its length parallel to the x axis. Cut planes are then set in 10mm intervals to find the cross section. Example of cross sections are given below in Fig.1:

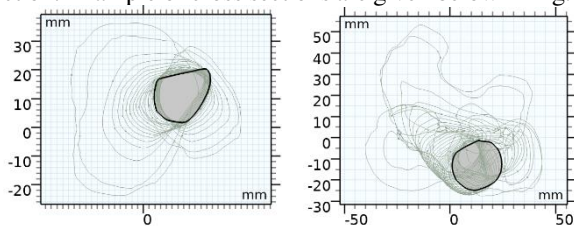


Figure 1: examples of midshaft cross sections in the tibia (left) and femur (right).

The simple models were generated using COMSOL's standard geometry builder. A set of standard parameters were chosen to allow for fair comparison of the models, given in Table 1. The material properties were selected to give an estimation of cortical bone material. The models were also emulated in MATLAB 2018a using the Timoshenko model (1) to give a level of verification of the results using these same parameters. Each cross-section shape in this study will have the same area to maintain consistency.

Table 1. Standard parameters of test rods

Variable	Value [Unit]
Length	0.8 [m]
Radius ¹	0.02 [m]
Cross-Sectional Area	0.00126 [m ²]

¹ Or equivalent metric – See Table 2.

Elastic Modulus	22 [GPa]
Density	2090 [kg/m ³]
Poisson Ratio	0.3 [N/A]
Maximum Element Length ²	0.02 [m]

3.1 Cross Sections

From observing the cross sections of the tibia and femur, it can be seen that their shape changes from circular to angular and with definite major and minor axes. Therefore, the following shapes in Table 2 were chosen to change from the symmetric circle to the asymmetric angular triangle. The circular prism is the simplest cross section and appears often in the literature [9,10]. As it is symmetric, $I_y = I_z$ and the modal frequencies repeat in perpendicular directions producing only one harmonic series. Triangular cross sections have been suggested previously [11] but there has been a lack of progress on investigating the theoretical shear coefficients and shape factors [12,13]. Given the verification of the COMSOL model for the other cross-sections, we investigated triangular cross-sections other than equilateral i.e. saline. A parameter sweep was carried out in MATLAB and COMSOL between the parameters in Table 2.

Table 2: Cross-sectional shapes and key parameters.

Shape	Parameters
Circle	Radius
Ellipse	Radius A; Radius B; A:B Ratio
Triangular - Equilateral	Side Length
Triangular - Saline	Circumcircle Radius; Internal angle

The circumcircle describes the circle which passes through all the vertices of a polygon, in this case the triangle. This is defined mathematically using sine rule:

$$2R = \frac{a}{\sin A} = \frac{b}{\sin B} = \frac{c}{\sin C} \quad (4)$$

Where:

R is the radius of the circumcircle, A , B & C are the angles of the triangle and a , b & c are the sides opposite those angles. Internal angle describes one of these angles A , B , & C as a variable. The remaining two angles are then adjusted

² COMSOL only.

to ensure the total sum is 180° . These two parameters are illustrated in Figure 2 below.

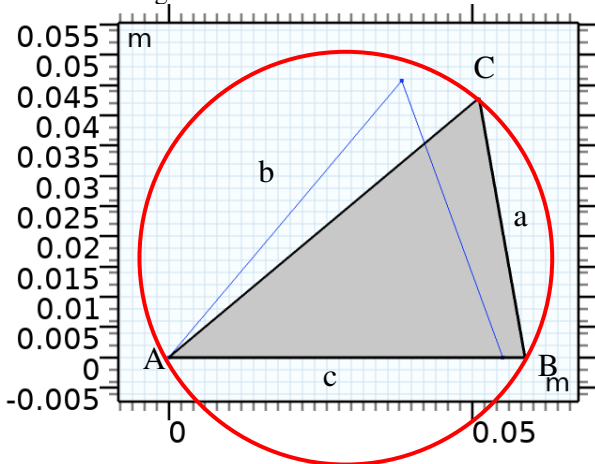


Figure 2: The saline triangle cross section showing the internal angles and sides for two triangles at 50° and 40° and the circumcircle in red for the 40° triangle. In the parameter sweeps, the angle A is varied.

The eigenfrequencies of the tibia and femur models were calculated using the eigenfrequency study in COMSOL's solid mechanics module. The same study was used with 3D models of the cross-sections listed in Table 2. A selected number of eigenfrequencies and their error to the MATLAB calculations are given in Table 3.

Table 3: Cross-sectional shape and modal frequencies

Shape	COMSOL F_1 - F_3 [Hz]	MATLAB Error %
Femur	[258.74/299.57/613.42]	-
Tibia	[365.96/455.62/1175.1]	-
Circle	[2x 179.34/2x 488.65/2x 942.33]	[0.002/0.011/0.023]
Ellipse	[120.02/266.85/329.10]	[-0.006/0.024/-0.006]
Triangle - E	[2x 196.81/2x 533.96/978.17]	[-0.006/-0.006/-0.022]
Triangle - 50°	[175.19/220.98/476.59]	[1.12/-35.64/3.13]
Triangle - 40°	[154.37/250.39/420.80]	[1.89/-76.53/5.54]

Triangle - 30°	[132.74/290.18/362.45]	[-10.00/-106.12/-26.26]
-----------------------	------------------------	-------------------------

The repeated modal frequencies of the circle and equilateral triangle are expected given the similar area moments in the two bending directions for those shapes. As seen in Figure 3, an asymmetric shape such as the ellipse allows for separate bending modes in the two directions with different area moments. A large error between the COMSOL and MATLAB results for the saline triangle is from the shear correction factor being unknown for this shape. For this cross-section, the COMSOL results are taken as the reference and the MATLAB results being the comparator, using a shear correction factor of $k_y = k_z = 0.73$ as used for the equilateral triangle [10] in equation (1).

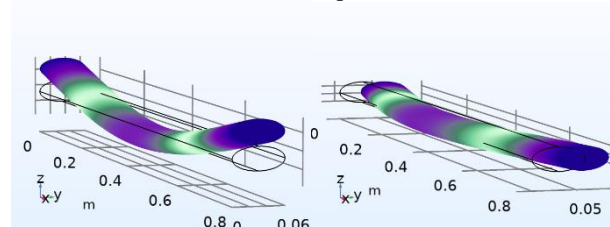


Figure 3: F_1 (left) and F_2 (Right) of the ellipse (A:B ratio of 1.5) showing the two bending directions in the z and y directions respectively.

Figure 4 shows the normalised frequencies of the real bone as circular markers and the different cross-section shape results as crosses, showing the modal frequency pattern for each shape. Referring to the triangular shape of the midshaft of the tibia in Figure 1, the triangular cross section of 50° is closer to the modal distribution of the tibia. The modal distribution has an average error across all normalised modes of 6.05%, while the ellipse has an average error of 34.43%

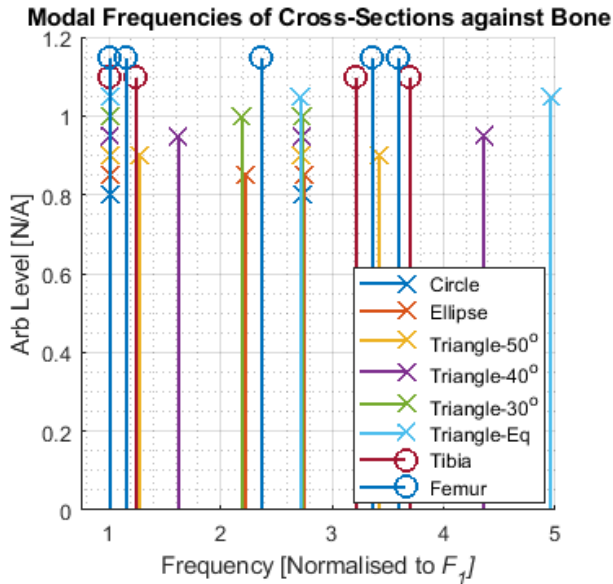


Figure 4: Normalised modal frequencies of cross-sections [crosses], tibia, and femur [circles].

The ellipse is one of the shapes with an asymmetrical cross section but the degree of symmetry can be adjusted through the A:B ratio. This is swept in Table 4 with the resulting modal frequency changes.

Table 4: Elliptical ratio change on modal frequencies

A:B Ratio	F_1-F_3 [Hz]	Change % [from 1.0]
1.0	[2x 179.34/ 2x 488.65/2x 942.33]	-
1.2	[149.76/214.60/409.46]	[16.50/ -19.66/16.21]
1.4	[128.52/249.53/352.13]	[28.34/ -39.14/27.93]
1.6	[112.56/284.10/308.83]	[37.24/ -58.41/36.80]
1.8	[100.10/274.90/318.28]	[44.19/ -55.28/34.86]

Changing the ellipse ratio splits the modal frequencies as the area moment changes in the two bending directions. The 1st bending modal frequency falls by over 25% once the

A:B ratio is 1.4, with the 2nd bending mode increasing in frequency to almost 40% compared to the circle.

The angle A in the saline triangle is swept from 60° to 30° in COMSOL which morphs the cross-section from equilateral to right-angled triangle. The results of this sweep are in Table 5.

Table 5: Angle change on modal frequencies

Angle 1 [deg]	F_1-F_3 [Hz]	Change % [from 60°]
60	[2x 196.81/2x 533.96/978.18]	-
50	[175.19/220.98/476.59]	[10.98/ -12.28/10.74]
40	[154.37/250.39/420.81]	[21.56/ -27.23/21.19]
30	[132.74/290.18/362.45]	[32.55/ -47.45/32.12]

As for the ellipse, the splitting of the modal frequencies are apparent but with clearer trend in the falling modal frequencies for 1st and 3rd modes. There is a greater % change in the modal frequencies for the 2nd bending mode, owing to the greater change in I_y compared to I_x .

3.2 Twist

We can implement a twist to the geometry in COMSOL which extrudes and rotates the vertices of the geometry over a specified distance. This implementation can reduce the cross-section area within the length of the prism, especially at twists greater than 45°. This can be seen in Figure 5 with the areas at the ends of the geometry (red circle) and the cross-section in the middle of the prism (yellow circle). Table 6 shows the amount of area reduction for some twist angles.

Table 6. Area Reductions for Twist Angles

Angle [deg]	Area [m ²]	Percent
0	0.0012524	100
22.5	0.0012047	96.191
45	0.0010690	85.356
90	0.00062617	49.998

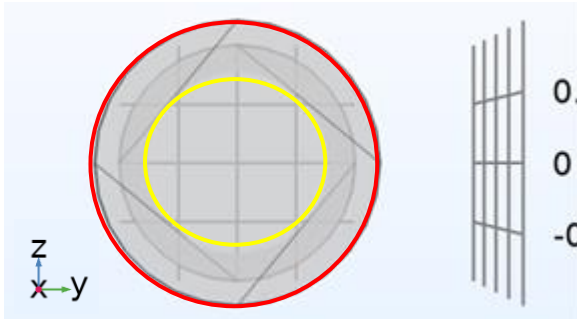


Figure 5: Geometry of the circle with a 90° twist showing the smaller cross-sectional area in the middle (yellow circle) compared to the ends (red circle).

Therefore, the twist will have a compounding effect of changing the cross-section along the length. The results of a few case examples are given in Table 7.

Table 7: Cross-section with twist modal frequencies

Shape	Twist [deg]	F_1 - F_3 [Hz]
Circle	0	[281.45/766.76/1478.41]
Circle	40	[259.70/722.82/1407.63]
Ellipse	40	[174.36/370.74/509.60]
Triangle - E	40	[285.60/795.52/1551.88]
Triangle - F 50	40	[254.46/319.28/714.94]
Triangle - F 40	40	[223.84/358.31/632.06]

The inclusion of twist gives a proportional reduction of the modal frequencies across all the cross-section shapes and mode number i.e. a twist of 20° gives a 1.5 to 2.5% decrease in the modal frequencies for all the cross sectional shapes. Further twist produces an increasing decrease in modal frequencies compared to the untwisted state. Twists of 30° produced a 4.4% to 2.7% decrease in modal frequencies for the triangular cross-sections for example. These values become 28.8% to 17.8% for a twist of 80° . Only the ellipse breaks this trend: for its lateral mode the modal frequency decreases by about 3% per 10° twist, and not only has a change of 9.7% for an extreme twist of 80° . But there are some exceptions given the influence of other effects such as the triangular internal angle or change in cross-sectional shape which can be investigated further.

3.3 Scale

To emulate the ends of the tibia and femur, the ends of the rod were given greater cross-sections than the midshaft. The two end faces of the midshaft are extruded with L_D and L_P for the distal and proximal ends respectively. The ends' cross-sections are increased with a scaling factor S_D and S_P and the geometry joins the midshaft face to the expanded end faces over the distance L_D and L_P (see Fig 6 for illustration).

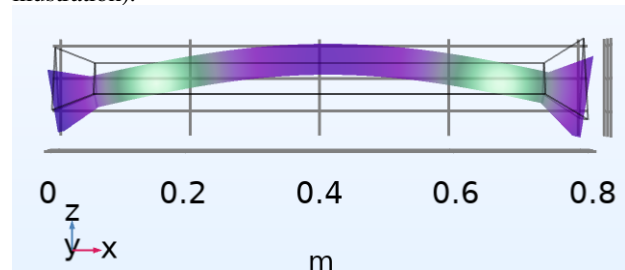


Figure 6: A triangular prism bending mode with the two ends with different scales S_D & S_P over L_D & L_P .

This creates a linear increase in the cross-sectional area which emulates the real bone's larger proximal and distal ends but ignores the change in cross-sectional shape at these ends. The ends of the model are adjusted separately to reflect the difference in size and extend of the proximal and distal end of the bone. The cross-section was kept as equilateral triangle for this experiment. The results of sweeping L_P , L_D , S_D and S_P are given in Table 9.

Table 9: Cross-section and scale on modal frequencies

L_P [m]	L_D [m]	S_P	S_D	F_1 - F_4 [Hz]
0.06 0	0.06 0	1	1	[309.18/309.20/840.87/841.08]
0.06 0	0.06 0	2	1	[277.57/278.05/780.10/781.04]
0.06 0	0.06 0	2	2	[248.90/250.20/718.05/718.79]
0.01 6	0.06 0	2	1	[277.48/277.93/778.98/779.93]
0.01 6	0.01 6	2	1	[268.68/269.47/780.23/781.66]
0.01 6	0.01 6	2	2	[231.36/233.31/708.66/7020.28]

Changing the scale of the cross sections at either end can decrease the frequencies by 1.1% to 2.3% depending on the mode number, to a total of 12% scaling from 1 to 2 times the midshaft cross-sectional area. Extending the length of the ends decreases the first two modal frequencies by 3% but the greater modes are less affected by the change of the end length or changing the cross-sectional area of the ends.

4. DISCUSSION

Much of the literature on modelling bone vibration makes assumptions on the cross-sectional shape and other physical features in order to simplify the problem and to allow comparison between types of bones and across studies. The cross sections chosen in this paper were inspired both by the physical shape of the bone but also what appeared in previous research. Of these shapes, both the circular and the equilateral triangle have repeated modes which are not apparent in the real bones as these shapes have axial symmetry in each of its bending directions. Only the ellipse and the non-equilateral triangle had the necessary differences in moments of inertia which allow for different modal frequencies for different bending directions. Changing the A:B ratio and the internal angle allowed for further fine tuning of the modal frequencies to better match the real bone eigenfrequencies, but the other factors of scale and twist will be needed to be incorporated together to achieve better closeness.

One of the goals of this research was to join the analytical modeling and FE techniques to allow for the benefits of both in the analysis of bone vibration. The key application of this can be in generating datasets for sensitivity studies into shape without needing to calculate for entire bones. Some of these features would require extensive modification of the analytical models to be accounted for, while FE methods can calculate the effects of these features much quicker and with fine variation possible. In the case of the saline triangle, this approach can inform further analytical development using FE methods to experiment with cross-sectional shapes in the first instance.

5. CONCLUDING REMARKS

This paper identified a few of the major physical features of the long bone (shape, cross-section, twist, and scale) to investigate their influence on the modal frequencies using FE modeling. Results showed that the symmetrical cross-sections such as the circle and equilateral triangle had

repeated modes not seen in real bone, while the saline triangle modal frequencies were closer to the tibia and femur (6% and 14% average error to normalised modal frequencies respectively). Twist decreased all modal frequencies from 10% to 5% per 10° with a few exceptions. Scaling the distal and proximal ends larger than the midshaft only decreased frequencies by 2.3% to 1.5% while making the scaled ends longer only dropped the modal frequencies by 3%. Further investigation is needed to understand if there are further parameters and features which have an effect on the modal frequencies in the shape of bone, as well as further exploration into the features covered in this paper.

6. REFERENCES

- [1] P. A. Arnold, E. R. Ellerbrock, L. Bowman, and A. B. Loucks, "Accuracy and reproducibility of bending stiffness measurements by mechanical response tissue analysis in artificial human ulnas," *Journal of Biomechanics*, vol. 47, no. 14, pp. 3580-3583, 2014/11/07/ 2014.
- [2] S. G. Roberts, T. M. Hutchinson, S. B. Arnaud, B. J. Kiratli, R. B. Martin, and C. R. Steele, "Noninvasive determination of bone mechanical properties using vibration response: A refined model and validation in vivo," *Journal of Biomechanics*, vol. 29, no. 1, pp. 91-98, 1996/01/01/ 1996.
- [3] B. Couteau, M.-C. Hobatho, R. Darmana, J.-C. Brignola, and J.-Y. Arlaud, "Finite element modelling of the vibrational behaviour of the human femur using CT-based individualized geometrical and material properties," *Journal of Biomechanics*, vol. 31, no. 4, pp. 383-386, 1998/04/01/ 1998.
- [4] R. L. Piziali, T. K. Hight, and D. A. Nagel, "An extended structural analysis of long bones—Application to the human tibia," *Journal of Biomechanics*, vol. 9, no. 11, pp. 695-701, 1976/01/01/ 1976.
- [5] J. J. Thomsen, "Modelling human tibia structural vibrations," *Journal of Biomechanics*, vol. 23, no. 3, pp. 215-228, 1990/01/01/ 1990.
- [6] G. Leon and H.-L. Chen, "Direct Determination of Dynamic Elastic Modulus and Poisson's Ratio of Timoshenko Rods," *Vibration*, vol. 2, no. 1, pp. 157-173, 2019. [Online].

- [7] E. Bauer. "Human Femur." <https://sketchfab.com/3d-models/human-femur-a9c1f1a88b104c3fbfe975fa10b31b31> (accessed 2023).
- [8] E. Bauer. "Human Tibia." <https://sketchfab.com/3d-models/human-tibia-7c1979d6127749bc80a9d9276d24edcd> (accessed 2023).
- [9] G. Lowet, R. Van Audekercke, G. Van der Perre, P. Geusens, J. Dequeker, and J. Lammens, "The relation between resonant frequencies and torsional stiffness of long bones in vitro. Validation of a simple beam model," *Journal of Biomechanics*, vol. 26, no. 6, pp. 689-696, 1993/06/01/ 1993.
- [10] J. M. Jurist and K. Kianian, "Three models of the vibrating ulna," *Journal of Biomechanics*, vol. 6, no. 4, pp. 331-342, 1973/07/01/ 1973.
- [11] R. J. Collier, O. Nadav, and T. G. Thomas, "The mechanical resonances of a human tibia: Part I—In vitro," *Journal of Biomechanics*, vol. 15, no. 8, pp. 545-553, 1982/01/01/ 1982.
- [12] J. Freund and A. Karakoç, "Shear and torsion correction factors of Timoshenko beam model for generic cross sections," *Res. Eng. Struct. Mater*, vol. 2, no. 1, pp. 19-27, 2016.
- [13] Z. Friedman and J. B. Kosmatka, "Torsion and flexure of a prismatic isotropic beam using the boundary element method," *Computers & Structures*, vol. 74, no. 4, pp. 479-494, 2000/02/01/ 2000.